J Appl Electrochem (2009) 39:2329–2335
DOI 10.1007/s10800-009-9917-z

ORIGINAL PAPER

Effects of antimony(III) on zinc electrodeposition from acidic sulfate electrolyte containing [BMIM]HSO_4

Qibo Zhang · Yixin Hua · Yan Li · QiFei Pei

Received: 26 February 2009 / Accepted: 26 April 2009 / Published online: 6 May 2009

Abstract The effect of antimony(III) on the cathodic current efficiency (CE), power consumption (PC), deposit morphology, and polarization behavior during electrodeposition of zinc from acidic sulfate solutions containing 1-butyl-3-methylimidazolium hydrogen sulfate-[BMIM]HSO_4 was investigated. The results indicated that the addition of Sb(III) alone decreased the CE, increased the PC, and deteriorated the quality of the zinc electrodeposits. However, the combined addition of Sb(III) and [BMIM]HSO_4 was found to be beneficial for zinc deposition and improved the surface morphology of the zinc electrodeposits. Maximum CE and minimum PC were obtained at the combined addition of 0.02 mg dm^{-3} Sb(III) and 5 mg dm^{-3} [BMIM]HSO_4. Depolarization of the cathode was noted in the presence of Sb(III) alone in the electrolyte whereas this effect was partly counteracted by the addition of [BMIM]HSO_4. Cathodic polarization curves were traced and analyzed to determine the electrokinetic parameters such as Tafel slope, transfer coefficient, and exchange current density so as to elucidate the nature of the electrode reactions. The data obtained from X-ray diffractogram revealed that the presence of Sb(III) did not change the structure of the electrodeposited zinc but affected the crystallographic orientation of the crystal planes.

Keywords Antimony(III) · Zinc · Deposit morphology · Crystal orientation · Ionic liquids

Q. Zhang · Y. Hua (✉) · Y. Li · Q. Pei
Faculty of Materials and Metallurgical Engineering, Kunming University of Science and Technology, Kunming 650093, China
e-mail: huayixin@gmail.com

1 Introduction

The zinc electrowinning process is very sensitive to the presence of impurities in the electrolyte. Neutral purification eliminates the bulk of the impurities, but in certain instances their concentrations still may be high enough to cause difficulties in zinc electrodeposition [1, 2]. Low levels of impurities greatly influence the cathodic deposition of zinc, leading to a decrease in current efficiency (CE) and to changes in deposit morphology [3] and cathodic polarization [4, 5]. By the addition of organic compounds to the electrolyte, it is possible to counteract the harmful effects of these metallic impurities and to produce zinc with high CE and good quality.

Over the past decades, the effects of numerous impurities such as cobalt and nickel [6–10], manganese [10–12], antimony [3–5, 13–16], copper [1, 8, 17, 18], iron [17, 18], cadmium [17], germanium [8, 15, 19, 20], and tin [21] on the CE and polarization behavior as well as their effects on deposit morphology and crystallographic orientations of the cathode during electrodeposition of zinc from acidic sulfate electrolyte have been studied. Although small concentrations of these impurities dramatically reduce the CE, their effects on deposit morphology and orientation as well as cathodic polarization are quite different. Therefore, a detailed study of their effect is necessary, which might provide insight into the general mechanism of impurity behavior.

Antimony(III), which has long been recognized as one of the most deleterious solution impurities for zinc electrodeposition whose presence in the electrolyte produces spongy and dark deposits [22]. Ault et al. [16] observed that Sb(III) had a very detrimental effect on coulombic efficiency and also exerted a strong grain-refining effect on the zinc deposit. Nevertheless, Sb(III) also plays a

beneficial role when combined with some organic additives producing optimum CE and acceptable surface morphology of the deposits [13, 23–29]. Mackinnon et al. [13] observed that certain combinations of Sb(III) and glue optimized the CE and consistently produced a (114) (112) (103) (102) (101) preferred deposit orientation. They also found a correlation between the CE values and the nucleation overpotential for zinc deposition. In a separate study [23] they studied the effects of saponin alone and in combination with Sb(III) and glue on the electrocrystallization of zinc from Kidd Creek zinc electrolyte. They observed that at optimum glue + Sb(III) levels, when saponin concentration $\geq$5 mg l^{-1} resulted in an increase in the CE and producing a smooth and uniform deposit. Tripathy et al. [22, 26–29] have studied the combination effect of Sb(III) and a series of organic additives on the electrowinning of zinc from acidic sulfate solution. They found that there were specific combinations of Sb(III) and these additives where the maximum in CE and minimum in power consumption (PC) as well as improved surface morphology were achieved. Similar observation was also obtained by Das et al. [24, 25].

In our pervious report [30], 1-butyl-3-methylimidazolium hydrogen sulfate ([BMIM]HSO_4) was found to be efficient as levelling agent. Thus, in the present study, a detailed investigation has been made to examine the effect of Sb(III) on the electrodeposition of zinc from sulfate solutions containing [BMIM]HSO_4. In addition, the role of Sb(III) and the synergistic effect with [BMIM]HSO_4 on the cathodic polarization behavior during the cathodic reduction process of Zn^{2+} ion was also investigated by electrochemical measurements and the kinetic parameters such as Tafel slope, transfer coefficient, and exchange current density for the electron transfer process were determined from the cathodic polarization curves to elucidate the nature of the electrode reactions.

2 Experimental details

2.1 Reagents

The zinc electrolyte was prepared from AnalaR zinc sulfate ($ZnSO_4 \cdot 7H_2O$) and analytical grade H_2SO_4. The antimony(III) concentration in the electrolytes was achieved by adding potassium antimony tartrate solution. 1-Butyl-3-methylimidazolium hydrogen sulfate ([BMIM]HSO_4) was laboratory synthesized as mentioned elsewhere [31, 32]. The electrolytic solution contained 55 g dm^{-3} zinc and 150 g dm^{-3} sulfuric acid and the specific experimental procedures were similar to as described previously [26].

2.2 Electrolysis

Small-scale galvanostatic electrolysis experiment was performed in a 250 cm^3 plexiglass cell. A pure (>99.95%) aluminum sheet and two parallel lead–silver–calcium–strontium alloy (Ag 0.2%, Ca and Sr 0.1–0.13%) plates of 5 cm^2 were used as the cathode and anode, respectively. The interelectrode distance was 2.5 cm. Zinc was deposited on both sides of the cathode onto a total area of 4.5 cm^2. All electrolysis experiments were run in a constant temperature bath at 40 ± 1 °C. In all cases, the current density was held constant at 400 A m^{-2} during the deposition time of 2 h. After electrolysis, the cathode was removed from the cell and washed thoroughly with distilled water and dried. The CE was calculated by weight according to Faraday's law.

2.3 Electrochemical measurements

A CHI760C electrochemical workstation (Shanghai CH Instruments Company, China) was used for electrochemical measurements. Electrochemical studies were based on the analysis of cyclic voltammetric measurements and potentiodynamic polarization tests. A conventional three-electrode cell was used for these experiments. All the measurements were preformed at 40 °C under atmospheric condition. The working electrode was made from high purity (>99.95%) aluminum and sealed with epoxy resin, with an effective area of 0.28 cm^2. A graphite rod was used as counter and a saturated calomel electrode (SCE) as the reference electrode. Cyclic voltammetric experiments were carried out by initiating scans at a constant scan rate of 10 mV s^{-1} from the initial potential of −0.70 V to the final potential of −1.25 V. The potentiodynamic polarization studies were carried out, after the cyclic voltametric tests, the potential was scanned from ca.−1.05 to −1.25 V with a constant scan rate of 5 mV s^{-1}. All potentials were recorded with respect to the SCE. Before each experiment, ultrapure argon was pumped into the electrolyte for 30 min to remove dissolved oxygen. The working electrode was polished with a sequence of emery papers of different grades (600, 800, and 1,200), degreased with anhydrous alcohol in an ultrasonic bath for 10 min, washed twice with distilled water, and finally dried.

2.4 Deposit examination

Sections of the zinc deposits were examined by scanning electron microscopy (SEM) using a Tescan VEGA II XMH microscope to determine the surface morphology of the deposit. A Rigaku D/max 2200 X-ray diffractometer was used to examine the preferred crystal orientations relative

to American Society for Testing and Materials (ASTM) standard for zinc powder.

3 Results and discussion

3.1 Cathode CE and PC

The effects of Sb(III) and in combination with $[BMIM]HSO_4$ on CE and PC during zinc electrodeposition from the zinc sulfate solution were studied. The results are listed in Table 1. As shown in this table, the CE has little change with the initial addition of Sb(III) but drops steadily at higher concentrations. In the additive-free solution, the CE is 90.8%. At 0.01 mg dm^{-3} Sb(III) the CE increases slightly to 91.3% and then falls gradually with the increase in the concentration of Sb(III). The effect is worst when the concentration of Sb(III) in the electrolysis is 0.08 mg dm^{-3}, causing a significant decrease in CE by ~23%. This initial increase in CE can be attributed to the catalytic effect of Sb(III) [24], in which both increases the rate of zinc deposition and hydrogen evolution, but at higher Sb(III) concentrations the hydrogen evolution reaction becomes dominant, so the CE of zinc decreases. $[BMIM]HSO_4$ is an effective levelling agent for zinc deposition from sulfate solution in our pervious report [30]. Proper addition of this additive is observed to increase CE, reduce PC, and improve the surface morphology of zinc deposits. It is interested to found that there is a specific combination of Sb(III) and the additive where CE is actually maximum. The optimum combination of 0.02 mg dm^{-3} Sb(III) and 5 mg dm^{-3} $[BMIM]HSO_4$ results in the highest CE (94.7%). This increase in CE in the presence of both Sb(III) and $[BMIM]HSO_4$ may be explained as follows: there exists a strong interaction between H^+ and Zn^{2+} for each unit of available current at the cathode during zinc electrodeposition from acidic sulfate electrolytes [29]. Cachet et al. [33] explained this in terms of a model based on the competition between the autocatalytic production of adsorbed intermediate, Zn^+_{ads} and the adsorption of $H_{ads,}$ which acts as an inhibitor. The addition of Sb(III) interferes with the hydrogen adsorption by forming a volatile hydride in the double layer [34], thus preventing H_{ads} from acting as an inhibitor for the deposition of zinc. On the other hand, the hydrogen evolution can also be suppressed by blocking the active sites through cathodic adsorption of $[BMIM]HSO_4$ [30]. Therefore, the addition of Sb(III) at low concentrations to the solution containing $[BMIM]HSO_4$ increases the CE.

The PC in the absence and in the presence of Sb(III) alone and the combined addition of Sb(III) and $[BMIM]HSO_4$ in the electrolytes during the electrodeposition of zinc is also given in Table 1. As can be seen, with the addition of Sb(III) at low concentrations the PC has little change, whereas more PC is required for the electrodeposition process with increasing the concentration of Sb(III). In addition, this increase in PC is more pronounced at higher Sb(III) concentrations and may be attributed to the secondary hydrogen evolution reaction where some of the power is consumed for hydrogen ion reduction. This effect is also reflected in the drastically fall in the CE of zinc ion reduction. However, the PC is found to decline rapidly in the combined addition of Sb(III) and $[BMIM]HSO_4$. The maximum reduction in PC of ~151 $kWht^{-1}$ is obtained at the combined addition of 0.02 mg dm^{-3} Sb(III) and 5 mg dm^{-3} $[BMIM]HSO_4$. This mainly ascribes to the increase in CE and the inhibition of hydrogen evolution through cathodic adsorption of $[BMIM]HSO_4$ as discussed above.

Table 1 Effect of Sb(III) on current efficiency in the absence and in presence of $[BMIM]HSO_4$ during zinc electrodeposition

[Sb(III)]/ mg dm^{-3}	$[BMIM]HSO_4$/ mg dm^{-3}	CE/%	Cell voltage/V	PC/$kWht^{-1}$
0	0	90.8	2.89	2,611
0.01	0	91.3	2.88	2,588
0.02	0	90.5	2.87	2,601
0.04	0	85.8	2.87	2,744
0.08	0	68.2	2.86	3,440
0.01	5	93.4	2.85	2,503
0.02	5	94.7	2.84	2,460
0.04	5	91.5	2.84	2,546
0.01	10	92.6	2.86	2,534
0.02	10	93.5	2.86	2,509
0.04	10	90.4	2.85	2,586

3.2 Polarization studies

The effect of Sb(III) alone and its synergistic effect with $[BMIM]HSO_4$ on the cathodic electroreduction of Zn^{2+} ion from the acidic sulfate solution was investigated using cyclic voltammetrically (Figs. 1 and 2). The nucleation overpotential (NOP) which is the difference between the nucleation potential, E_{nu}, and the cross overpotential, is discussed in the previous report [28]. And the data of NOP can be determined from the cyclic voltammograms [35], which can be regarded as an indicator of the extent of polarization of a cathode [36]. The addition of Sb(III) depolarizes (decreases the NOP) the cathode during Zn^{2+} reduction on an aluminum substrate as this addition promoted a progressive shift of the deposition potential to more positive direction (Fig. 1) by comparing to the antimony-free electrolyte. For example, the NOP values obtained in the blank solution is 110 mV (Table 2).

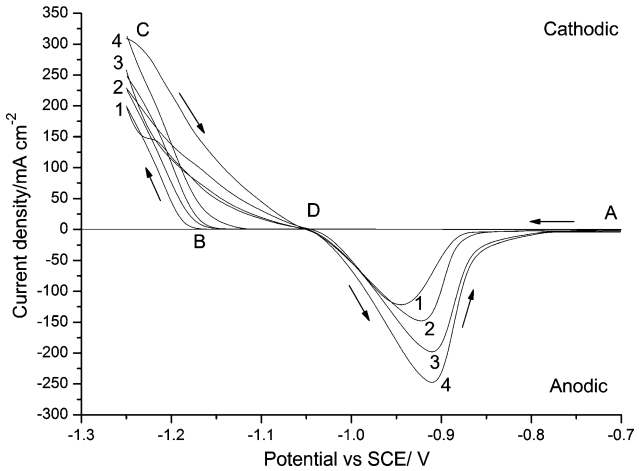

Fig. 1 Cyclic voltammograms of acidic zinc sulfate solutions in the presence of Sb(III). (1) Blank, (2) 0.01 mg dm^{-3}, (3) 0.02 mg dm^{-3}, and (4) 0.04 mg dm^{-3}

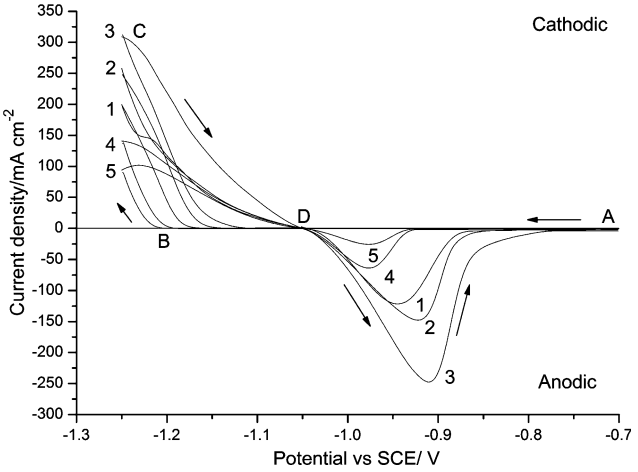

Fig. 2 Cyclic voltammograms of acidic zinc sulfate solutions in the presence of Sb(III) and [BMIM]HSO_4. (1) Blank, (2) 0.02 mg dm^{-3} Sb(III), (3) 0.04 mg dm^{-3} Sb(III), (4) [2] + 5 mg dm^{-3} [BMIM]HSO_4, and (5) [2] + 10 mg dm^{-3} [BMIM]HSO_4

Table 2 Effect of Sb(III) on nucleation potential (E_{nu}) and nucleation overpotetail (NOP) in the absence and in presence of [BMIM]HSO_4 during zinc electrodeposition

[Sb(III)]/mg dm^{-3}	[BMIM]HSO_4/mg dm^{-3}	$-E_{nu}$/mV	−NOP/mV
0	0	1,162	110
0.01	0	1,143	91
0.02	0	1,140	88
0.04	0	1,112	60
0.01	5	1,195	143
0.02	5	1,190	138
0.04	5	1,178	126
0.01	10	1,208	156
0.02	10	1,203	151
0.04	10	1,186	134

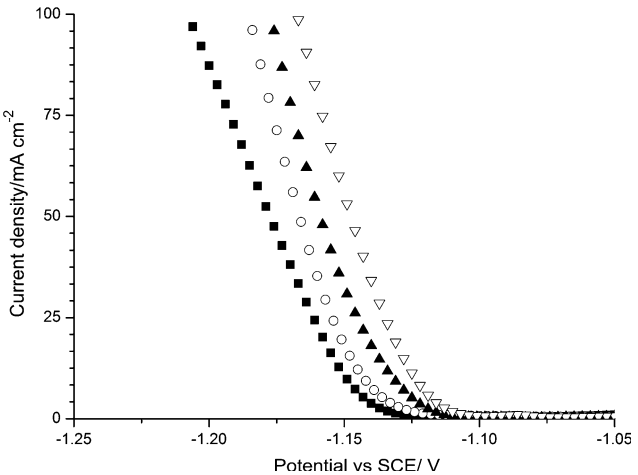

Fig. 3 Effect of Sb(III) on the cathodic polarization during zinc deposition on aluminum with different concentrations. (*Filled square*) blank, (*open circle*) 0.01, (*filled triangle*) 0.02, and (*open inverted triangle*) 0.04 mg dm^{-3}

Addition of 0.02 mg dm^{-3} Sb(III) causes a decrease in the NOP value to 88 mV. At 0.04 mg dm^{-3} Sb(III) the NOP value becomes 60 mV. The decrease in the NOP value is likely to increase the rate of zinc deposition as well as hydrogen evolution and this effect enhances with increase in the additive concentration. However, the combined addition of 0.02 mg dm^{-3} Sb(III) and 5 mg dm^{-3} [BMIM]HSO_4 increases the NOP from 110 to 138 mV and further increases to 151 mV (Fig. 2) with increasing the concentration of [BMIM]HSO_4 up to 10 mg dm^{-3}. Similar observation is also obtained when [BMIM]HSO_4 is added to the solution containing different concentrations of Sb(III). It is also clear that the addition of [BMIM]HSO_4 increases the NOP values substantially, along with the reduction of the cathodic peak current, denoting an inhibition of electrocrystallization (Fig. 2). This is generally attributed to the surface coverage of the cathode by a strongly adsorbed additive layer. Such a layer increases the interfacial viscosity and decreases the mass transfer [22]. This result also indicated that [BMIM]HSO_4 partly counteract the effect of Sb(III) causing a balanced effect.

The cathodic potentiodynamic polarization curves for zinc electrodeposition on aluminum electrode from acidic zinc sulfate solutions in the absence and in the presence of Sb(III) alone and in combination with [BMIM]HSO_4 are presented in Figs. 3 and 4. It can be seen that an increase in the Sb(III) concentration progressively increases the electroreduction potential of Zn^{2+} ion (Fig. 3). This depolarizing effect could be due to the increase in the rate of electron transfer for both Zn^{2+} and H^+ reduction. Moreover, the polarization behavior of the zinc deposition in the

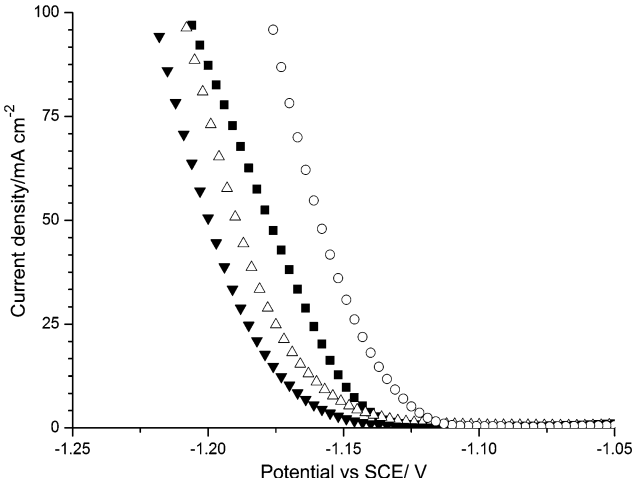

Fig. 4 Effect of Sb(III) and [BMIM]HSO_4 on the cathodic polarization during zinc deposition on aluminum. (*Filled square*) blank, (*open circle*) 0.02 mg dm^{-3} Sb(III), (*open triangle*) 0.02 mg dm^{-3} Sb(III) + 5 mg dm^{-3} [BMIM]HSO_4, and (*filled inverted triangle*) 0.02 mg dm^{-3} Sb(III) + 10 mg dm^{-3} [BMIM]HSO_4

presence of both Sb(III) and [BMIM]HSO_4 in the electrolyte is consistent with the results obtained by cyclic voltammetry (Fig. 4).

The kinetic parameters Tafel slope, b (mV decade^{-1}), transfer coefficient, α, and exchange current densities, i_0 (mA cm^{-2}), for zinc electrodeposition on aluminum electrode were calculated from their respective cathodic polarization curves using the same method as reported earlier [28, 30]. The results are given in Table 3. The marked decrease in Tafel slopes with the addition of Sb(III) indicates that the charge transfer reaction is affected strongly by the presence of Sb(III) in the solution, and this effect is more pronounced with increasing Sb(III) concentrations. This is conformed by significantly increasing of transfer coefficient when Sb(III) is present in the solution. This change is probably due to the hydrogen evolution reaction occurring along with the zinc deposition process. Meanwhile, the increase in exchange current density in the presence of Sb(III) may be attributed to the secondary hydrogen evolution. Addition of [BMIM]HSO_4 to the antimony-containing solutions does not have significant effect on the Tafel slopes and transfer coefficients, indicating that it do not control the charge transfer reaction and have no effect on the symmetry of the electron transfer reaction, respectively. However, the presence of [BMIM]HSO_4 has an inhibiting effect on the kinetics of the zinc discharge process, indicated by the decrease of the i_0, which can be attributed to its adsorption at the cathodic electrode surface. This adsorption results the blocking of the active nucleation sites of the cathode surface. In addition, the progressive decrease in i_0 with increasing the concentration of [BMIM]HSO_4 could be related to the strong adsorption of this additive on the cathode. Changes in kinetic parameters are also reflected in CE, PC, and NOP values.

3.3 Deposit morphology and orientation

The zinc deposits obtained were of high purity (99.99%) without any contamination of Sb and were examined using SEM and X-ray diffraction to determine the surface morphology and crystallographic orientations, respectively. Typical SEM photomicrographs are shown in Fig. 5 and the crystallographic orientations of zinc deposits in the absence and in presence of Sb(III) alone and the presence of both Sb(III) and [BMIM]HSO_4 are given in Table 4.

As it can be seen from Fig. 5b and c, the addition of Sb(III) significantly changed the morphology of the zinc deposits as compared with those obtained from solutions without additives (Fig. 5a). The zinc deposit obtained from addition-free electrolyte is bright but not smooth. The trace addition of Sb(III) even at parts per billion level deteriorated the quality of the deposits, which results in a dark and curly deposit (Fig. 5b). At higher concentration of Sb(III), the deposit obtained is spongy and the corrosion became more evident with zinc dissolving away leaving rough crystallites behind (Fig. 5c). This morphology type seems

Table 3 Effects of Sb(III) on the kinetic parameters in the absence and in presence of [BMIM]HSO_4 during zinc electrodeposition from acidic sulfate solution

[Sb(III)]/ mg dm^{-3}	[BMIM]HSO_4/ mg dm^{-3}	Tafel slope/ mV per decade	Transfer coefficient, α_c	Exchange current density, i_0/mA cm^{-2} ($\times 10^{-2}$)
0	0	127	0.49	39.3
0.01	0	83	0.75	48.6
0.02	0	71	0.87	59.1
0.04	0	67	0.93	85.5
0.01	5	86	0.72	33.0
0.02	5	74	0.82	42.9
0.04	5	66	0.94	71.5
0.01	10	88	0.70	22.8
0.02	10	72	0.86	37.3
0.04	10	67	0.93	65.6

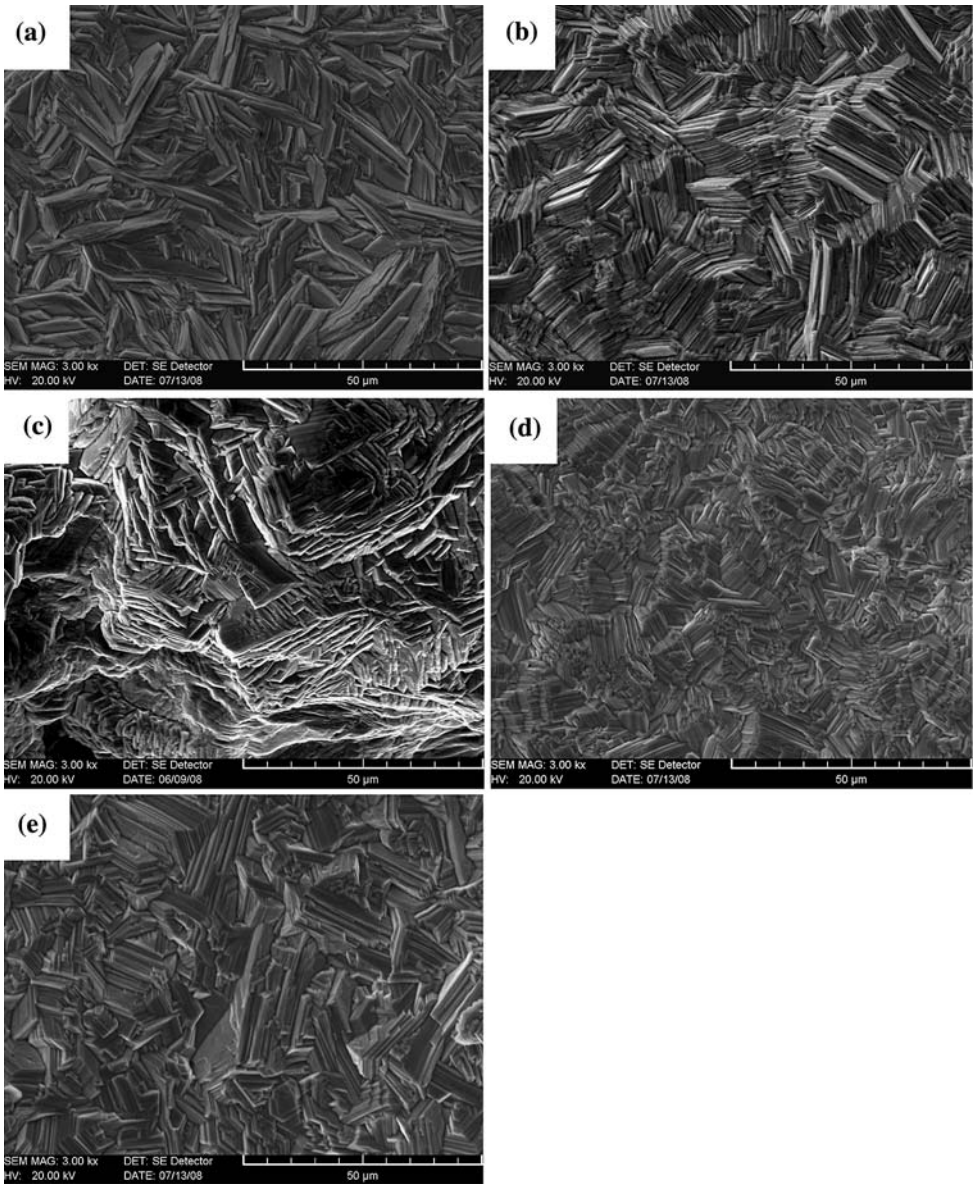

Fig. 5 Scanning electron micrographs of zinc deposits. **a** Blank, **b** 0.02 mg dm^{-3} Sb(III), **c** 0.08 mg dm^{-3} Sb(III), **d** 0.02 mg dm^{-3} Sb(III) + 5 mg dm^{-3} $[BMIM]HSO_4$, and **e** 0.08 mg dm^{-3} Sb(III) + 5 mg dm^{-3} $[BMIM]HSO_4$

Table 4 Effects of Sb(III) on crystallographic orientations of zinc deposits in the absence and in presence of $[BMIM]HSO_4$

[Sb(III)]/ mg dm^{-3}	$[BMIM]HSO_4$/ mg dm^{-3}	Crystallographic orientations (*hkl*) and peak intensity ratio (I/I_{max})/%							
		(002)	(100)	(101)	(102)	(103)	(110)	(112)	(201)
0	0	–	11	100	6	2	3	12	18
0.01	0	11	8	100	26	4	3	13	9
0.02	0	9	9	100	15	5	3	14	6
0.04	0	9	11	100	20	3	5	13	10
0.01	5	6	6	100	25	4	3	7	3
0.01	10	6	4	100	23	5	4	6	3
0.02	5	5	3	100	21	7	4	8	4
0.02	10	4	1	100	27	7	3	6	3

to facilitate hydrogen evolution. However, addition of Sb(III) at low concentration (0.02 mg dm^{-3}) to the solutions containing $[BMIM]HSO_4$ reduces the platelet size producing a smooth and compact deposit (Fig. 5d, e), showing a synergistic effect of the two additives as discussed in the previous section.

With regard to crystallographic orientations, the zinc deposit obtained from addition-free electrolyte consists of hexagonal platelets of moderate size with (101) (201) (112) (100) as the order of preferred crystal orientations. The addition of 0.01 mg dm^{-3} Sb(III) causes a significant increase in the peak intensity of (102) and (002) crystal planes and results (101) (102) (112) (002) as the preferred orientation. The crystal orientations are remained almost the same with increase in the concentrations of Sb(III). In addition, the combined addition of Sb(III) and $[BMIM]HSO_4$ in the electrolyte also resulted changes in the orientation, and such changes appeared to be different from those obtained with Sb(III). For example, addition of 0.02 mg dm^{-3} Sb(III) to the solution containing 5 mg dm^{-3} $[BMIM]HSO_4$, the crystallite growth in the direction of (201) (100) (112) is inhibited and the order changes to (101) (102) (112) (103) accompanied with reduction in the size of the crystallites. Similar observations are obtained with increasing the concentration of $[BMIM]HSO_4$ to 10 mg dm^{-3}. The orders of preferred crystal orientation do not change much, and in all cases (101) is found to be the most preferred orientation.

4 Conclusions

The effect of Sb(III) alone and its combined addition with $[BMIM]HSO_4$ on zinc electrodeposition from acidic sulfate solutions has been investigated and the conclusions drawn from the results are summarized as follows.

(i) The CE of zinc electrodeposition from acidic zinc sulfate solution increases with reduction in PC in the presence of low concentration of Sb(III), however, decrease in CE (increase in PC) is observed at higher Sb(III) ($\geq$0.04 mg dm^{-3}) concentrations.

(ii) The combined addition of Sb(III) and $[BMIM]HSO_4$ is found to be beneficial for zinc deposition and the maximum CE and minimum PC are obtained at the combined addition of 0.02 mg dm^{-3} Sb(III) and 5 mg dm^{-3} $[BMIM]HSO_4$.

(iii) Addition of Sb(III) in the electrolyte causes depolarization of the cathode during the electroreduction of Zn^{2+}. This effect is partly counteracted by the addition of $[BMIM]HSO_4$ leading a balanced effect.

(iv) The antimony-containing electrolytes deteriorate the morphology of the electrodeposited zinc. In particular, at higher concentration of Sb(III) a spongy with corroded deposit is obtained. However, an optimum combined addition of Sb(III) and $[BMIM]HSO_4$ produces a smooth, compact, and fine-grained deposit.

(v) The presence of Sb(III) alone and in combination with $[BMIM]HSO_4$ do not change the structure of the electrodeposited zinc but affect the preferred crystallographic orientations of the crystal planes.

Acknowledgements The authors thank XinSheng Li for assistance in SEM and gratefully acknowledge the financial support of the National Natural Science Foundation of China (Project No.50564006) and the Natural Science Foundation of Yunnan Province (Project No.2005E0004Z).

References

1. Mackinnon DJ (1985) J Appl Electrochem 15:953
2. Mackinnon DJ, Brannen JM, Fenn PL (1987) J Appl Electrochem 17:1129
3. Robinson DJ, O'Keefe TJ (1976) J Appl Electrochem 6:1
4. MacKinnon DJ, Brannen JM (1977) J Appl Electrochem 7:451
5. Lamping BA, O'Keefe TJ (1976) Metall Trans 7B:551
6. Maja M, Spinelli P (1971) J Electrochem Soc 118:1538
7. Wark IW (1979) J Appl Electrochem 9:721
8. Maja M, Penazzi N, Fratesi R, Roventi G (1982) J Electrochem Soc 129:2695
9. Mackinnon DJ, Morrison RM, Brannen JM (1986) J Appl Electrochem 16:53
10. Stefanov Y, Vane I (2002) Hydrometallurgy 64:193
11. Mackinnon DJ, Brannen JM (1991) Hydrometallurgy 27:99
12. Mackinnon DJ (1994) Hydrometallurgy 35:11
13. Mackinnon DJ, Morrison RM, Mouland JE, Warren PE (1990) J Appl Electrochem 20:728
14. Turomshina UF, Stender VV (1955) J Appl Chem USSR 28:347
15. Fosnacht DR, O'Keefe TJ (1983) Met Trans 14B:645
16. Ault AR, Frazer EJ (1988) J Appl Electrochem 18:583
17. Muresan L, Maurin G, Oniciu L, Gaga D (1996) Hydrometallurgy 43:345
18. Saba AE, Elsherief AE (2000) Hydrometallurgy 54:91
19. Fosnacht DR, O'Keefe TJ (1980) J Appl Electrochem 10:495
20. Mackinnon DJ, Fenn PL (1984) J Appl Electrochem 14:467
21. Mackinnon DJ, Fenn PL (1984) J Appl Electrochem 14:701
22. Tripathy BC, Das SC, Singh P, Hefter GT, Misra VN (2004) J Electroanal Chem 565:49
23. Mackinnon DJ, Morrison RM, Mouland JE, Warren PE (1990) J Appl Electrochem 20:955
24. Das SC, Singh P, Hefter GT (1996) J Appl Electrochem 26:1245
25. Das SC, Singh P, Hefter GT (1997) J Appl Electrochem 27:738
26. Tripathy BC, Das SC, Singh P, Hefter GT (1997) J Appl Electrochem 27:673
27. Tripathy BC, Das SC, Singh P, Hefter GT (1999) J Appl Electrochem 29:1229
28. Tripathy BC, Das SC, Hefter GT, Singh P (1998) J Appl Electrochem 28:915
29. Tripathy BC, Das SC, Misra VN (2003) Hydrometallurgy 69:81
30. Zhang QB, Hua YX (2009) J Appl Electrochem 39:261
31. Huddleston JG, Visser AE, Reichert WM, Willauer HD, Broker GA, Rogers RD (2001) Green Chem 3:156
32. Whitehead JA, Lawrance GA, McCluskey A (2004) Aust J Chem 57:151
33. Cachet C, Wiart R (1990) J Appl Electrochem 20:1009
34. Turomshina UF, Stender VV (1955) J Appl Chem USSR 28:151, 347, 447
35. Mohanty US, Tripathy BC, Singh P, Das SC (2001) J Appl Electrochem 31:579
36. Mohanty US, Tripathy BC, Singh P, Das SC (2001) J Appl Electrochem 31:969